Nanoceria quantification based on its oxidative effect towards the ferrocyanide/ferricyanide system

Alba Iglesias-Mayor[a], Lucía Fernández-Murillo[b], Francisco Javier García-Alonso[b]

Alfredo de la Escosura-Muñiz[a*], Agustín Costa-García[a*]

[a] *NanoBioAnalysis Group-Department of Physical and Analytical Chemistry, University of Oviedo, Julián Clavería 8, 33006, Oviedo, Spain*

[b] *NanoBioAnalysis Group-Department of Organic and Inorganic Chemistry, University of Oviedo, Julián Clavería 8, 33006, Oviedo, Spain*

**Corresponding author. E-mail address: alfredo.escosura@uniovi.es; costa@uniovi.es*

Phone: +34985103521; +34985103488

ABSTRACT

The present work reports for the first time a novel method for poly (acrylic acid)-coated nanoceria (PAA-CNPs) quantification based on its oxidative activity towards the $Fe(CN)_6^{3-/4-}$ red-ox system. Stable suspensions of 3 nm-sized PAA-CNPs were first prepared and characterized. It was found that the presence of PAA-CNPs on the electrode surface exerts a high oxidative effect on $Fe(CN)_6^{4-}$ before the voltammetric reduction, being that effect evident in acidic and neutral pH. Such behaviour allows the rapid and sensitive PAA-CNPs quantification taking advantage of the chronoamperometric mode. By applying a voltage of 0 V, the value of the current recorded at 10 s is proportional to the amount of PAA-CNPs deposited on screen-printed carbon electrodes (SPCEs). Under the optimized conditions, a detection limit as low as 3.15×10^{13} NPs/mL with a linear dynamic range between 3.71×10^{13} and 1.85×10^{15} NPs/mL and a reproducibility (RSD) of 4% is obtained. To the best of our knowledge, this is the first time that such property of PAA-CNPs is studied and applied for quantification purposes. Furthermore, the proposed detection method does not require the chemical agents used in most existing assays for the detection of NP tags. We envisage that this methodology could open the way to further use of PAA-CNPs tags in biosensing as advantageous alternative to enzymes.

KEYWORDS: Nanoceria; Oxidative effect; Electrochemistry; Chronoamperometry

1. Introduction

Cerium (Ce) atom ([Xe] $4f^1$ $5d^1$ $6s^2$) unlike the other lanthanides, has two oxidation states, existing as ceric (Ce^{4+}) or cerous (Ce^{3+}) ion **[1,2]**. As oxide, it is found in two forms: CeO_2 (Ce^{4+}) or Ce_2O_3 (Ce^{3+}) in bulk material **[3]**. Cerium oxide nanoparticles (CeO_{2-x} NPs, CNPs), also known as ceria nanoparticles or nanoceria display the classic cubic fluorite lattice. Although most of the Ce atoms are present as Ce^{4+} ions, the nanostructure usually contains a variable amount of Ce^{3+} ions in its surface as intrinsic defects. The ratio of cations (Ce^{3+}/ Ce^{4+}) is function of the particle size, being the Ce^{3+} content higher for smaller particles, and consequently higher the concentration of defects and oxygen vacancies **[4,5]**.

A wide range of techniques such as thermal decomposition **[6,7]**, aqueous precipitation **[8]** and reversed micelles **[9]** have been reported to synthesize CNPs, being their red-ox properties and biological activity highly dependent on the method used for the synthesis. CNPs have been synthesized both bare, in pure water **[10]**, or wrapped with a coating of a protective substance, such as polyethylene glycol **[11]**, dextran **[12]** or polyacrylic acid **[13]**, which are needed to prevent aggregation.

CNPs have physical and chemical properties like bulk material. However, many of their unique features, such as its potential as catalyst, are due to its high oxygen storage capacity combined with its fluorite structure and its ease of transition between +3 and +4 states, being the oxygen defects the preferential sites for oxidative reactions. Additionally, the relatively high abundance of these vacancies in CNPs is speculated to be responsible for the altered red-ox chemistry of the CNPs versus bulk CeO_2 **[14,15]**. CNPs stand out from other metal oxide nanoparticles due to the dual oxidation state of Ce at the NP, allowing it to take part in red-ox reactions both as oxidizing and reducing agents **[16]**. Red-ox reactions of the Ce (III)/Ce (IV) couple in aqueous acidic solutions

play an important role in electrochemical processes, being Ce (IV) a strong oxidant capable of easy electrochemically regenerate **[17]**.

Recently, it was found that CNPs among other NPs also show multi-bioenzyme mimetic properties, including catalase **[4]**, superoxide dismutase **[18,19]**, peroxidase **[20,21]** and phosphatase **[22]** mimetic properties. CNPs are a promising and fascinating material in biological fields such as in biomedicine **[23]**, bioanalysis **[13,24]**, bioscaffolding **[25,26]** and drug delivery **[27,28]**. They also have intrinsic oxidase-like activity, as they can quickly catalyse the oxidation of organic chromogenic substrates (e.g. TMB, ABTS) without any oxidizing agent (e.g. H_2O_2) **[29,30]**. That activity depends on the pH, the size as well as the coating thickness, in the case of polymer coated CNPs. Some studies had shown that its oxidase-like activity increased along with the decrease of the pH, behaving as a weak oxidant at neutral pH and as a strong at acidic pH **[31]**.

Another point to consider is the interaction of CNPs with red-ox active compounds. Apart from the case of H_2O_2, little is known about the interaction of CNPs with red-ox components. It has been discovered that both ascorbic and citric acid as well as phenolic compounds may work as reducing agents, reacting with the Ce^{4+} of the CNPs and converting it to Ce^{3+} **[16]**.

However, as far as we know, CNPs quantification methods have not ever been reported. In this context, we propose for the first time a method for CNPs electrochemical quantification. The method is very simple, taking advantage of the oxidative effect of PAA-CNPs towards the ferrocyanide/ferricyanide system. Moreover, our method does not require the chemical agents used in most existing assays for the detection of NP tags. We envisage that this methodology could open the way to further use of PAA-CNPs tags in biosensing as advantageous alternative to enzymes. Actually,

the easy PAA-CNPs functionalization via click chemistry has been previously reported **[30]**, demonstrating the feasibility of our purpose.

2. Experimental

2.1. Materials and instruments

Cerium (III) nitrate hexahydrate ($Ce(NO_3)_3 \cdot 6\ H_2O$), poly (acrylic acid) (PAA, 1.8 kDa), ammonia aqueous solution (28% in NH_3), phosphate buffer tablets (for 10 mM PBS pH 7.4), potassium hexacyanoferrate (II) trihydrate ($K_4Fe(CN)_6 \cdot 3H_2O$), potassium hexacyanoferrate (III) ($K_3Fe(CN)_6$), sodium acetate and cerium standard for ICP (1000 mg/L Ce in nitric acid) were obtained from Sigma-Aldrich (Spain). Amicon Ultra centrifugal filters (Ultra-4, MWCO 30 kDa) were purchased to Millipore (USA). Nylon membrane syringe filter (pore 0.45 µm, diam. 25 mm) and nitric acid were obtained from VWR international (USA). Hydrochloric acid fuming 37%, acetic acid (glacial) 100% anhydrous, sodium hydroxide and sodium chloride were purchased to Merck (Germany). Multifuge 3 L-R centrifuge from Heraeus (Germany), centrifuge model 2716 from Nahita (Spain), FT-IR Spectrometer Paragon 1000 from PerkinElmer (USA), Zetasizer Nano ZS system from Malvern Instruments (United Kingdom), JEM 2100 transmission electron microscope from JEOL (Japan), Triple Quadrupole Inductively Coupled Plasma Mass Spectrometer from Agilent Technologies (USA) were used for the PAA-CNPs preparation, characterization and quantification. Electrochemical measurements were performed with an Autolab PGSTAT-10 from Eco Chemie (The Netherlands), controlled by Autolab GPES software from Metrohm (Switzerland). Both screen-printed carbon electrodes (SPCEs, ref. DRP-110) and their connector for the potentiostat (ref. DRP-DSC) were purchased from DropSens S.L (Spain). The conventional three-electrode configuration of SPCEs includes both carbon

working and counter electrodes and a silver pseudoreference electrode. All measurements were carried out at room temperature.

2.2. Methods

2.2.1. Synthesis, purification and characterization of poly (acrylic acid) coated nanoceria (PAA- CNPs)

Synthesis of poly (acrylic acid)-coated nanoceria (PAA-CNPs) was performed as previously described **[30]** with some modifications. Briefly, 2 mL of a cerium (III) nitrate hexahydrate solution (0.436 g, 1 mmol) were mixed with 2 mL of a poly (acrylic acid solution (0.901 g, 0.5 mmol) and kept under continuous stirring for 24 h at room temperature. Then 1.0 mL of 7.9 M ammonia solution were added and stirred for 24 h. After centrifugation at 5000 rpm for 3 min, the supernatant solution was purified by successive centrifugations (4 ×) at 2600g for 45 min using a 30 KDa Amicon cell. Afterwards, the solution was centrifuged again at 8000 rpm for 5 min, followed by filtering and final storage at 4 °C.

HR-TEM and dynamic light scattering were used for PAA-CNPs characterization. Elemental quantification of Cerium from the NPs was carried out via external calibration by inductively coupled plasma mass spectrometry (ICP-MS).

2.2.2. Electrochemical measurements

10 µL of PAA-CNPs suspension were deposited on the working electrode and allowed to dry at room temperature. After that, 40 µL of the red-ox compound solution were added and the electrochemical measurements were performed. Cyclic voltammetry scans were recorded in the range from - 0.5 V to + 1.0 V for $Fe(CN)_6^{4-}$ and from + 1.0 V to - 0.5 V for the $Fe(CN)_6^{3-}$ at a scan rate of 50 mV/s. Scan rate studies were also performed varying the scan rate between 10 and 500 mV/s. Chronoamperometric scans

were performed applying a constant potential of 0 V for 60 s. All measurements were performed by triplicate without removing oxygen from the solution. A new electrode was used for each measurement.

3. Results and discussion

3.1. Characterization of PAA-CNPs

The size and shape of the synthesized PAA-CNPs was evaluated by HR-TEM. Spherical PAA-CNPs were observed, as shown in **Fig. 1A**. NP sizes were measured by counting with digital analysis using *ImageJ* software, giving an average diameter of 3 ± 1 nm (SD, *n* = 30) (**Fig. 1B**).

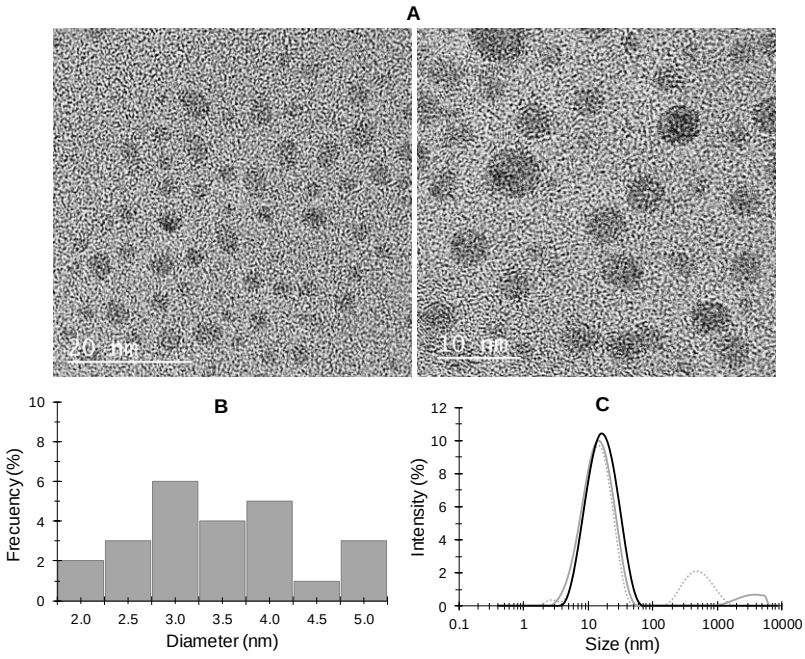

Fig. 1. (A) HR-TEM images at different magnifications and (B) nanoparticle size distribution histogram of the obtained PAA-CNPs. (C) DLS intensity size distribution graph for PAA-CNPs suspension before centrifugation (grey dotted line), after 5 min of centrifugation at 8000 rpm (grey solid line) and after filtration with a 0.45 µm pore-sized nylon filter (black line).

Such NPs are obtained after total removal of PAA and NH_4NO_3 by filtration (30 kDa). DLS analysis was also conducted for the determination of the polydispersity of the obtained suspension. Two main peaks were observed in the DLS plot at 16 nm and 563 nm hydrodynamic diameter (**Fig. 1C**, grey dotted line). The aggregates of 563 nm disappeared after 5 min of centrifugation at 8000 rpm, but a bigger cluster was formed meaning that the hydrodynamic diameter was about 3.3 μm (**Fig. 1C**, grey solid line). Finally, that cluster was removed passing the suspension through a nylon membrane syringe filter (0.45 μm pore diameter), appearing only one peak in the DLS image (**Fig. 1C**, black line).

On the other hand, the elemental concentration of cerium in the final NP suspension was 54 ± 1 ppm as quantified by ICP-MS. The NP concentration was estimated as 9.27×10^{16} NPs/mL considering PAA-CNPs as perfect spheres of 3 nm of diameter.

3.2. Oxidative effect of PAA-CNPs towards the $Fe(CN)_6^{3-/4-}$ red-ox system

Cyclic voltammograms (CVs) were recorded in 1 mM $K_4[Fe(CN)_6]$ and $K_3[Fe(CN)_6]$ solutions in different supporting electrolytes: acidic (0.1 M HCl), neutral (0.1 M NaCl) and basic (0.1 M NaOH) ones, for both bare and PAA-CNPs-modified electrodes. Background voltammograms were recorded for PAA-CNPs-modified electrodes in the supporting electrolyte without red-ox compound. As can be seen in **Fig. 2**, the currents measured in presence of PAA-CNPs (black voltammograms) are more negative than the ones obtained for the bare electrodes (grey voltammograms) in all cases.

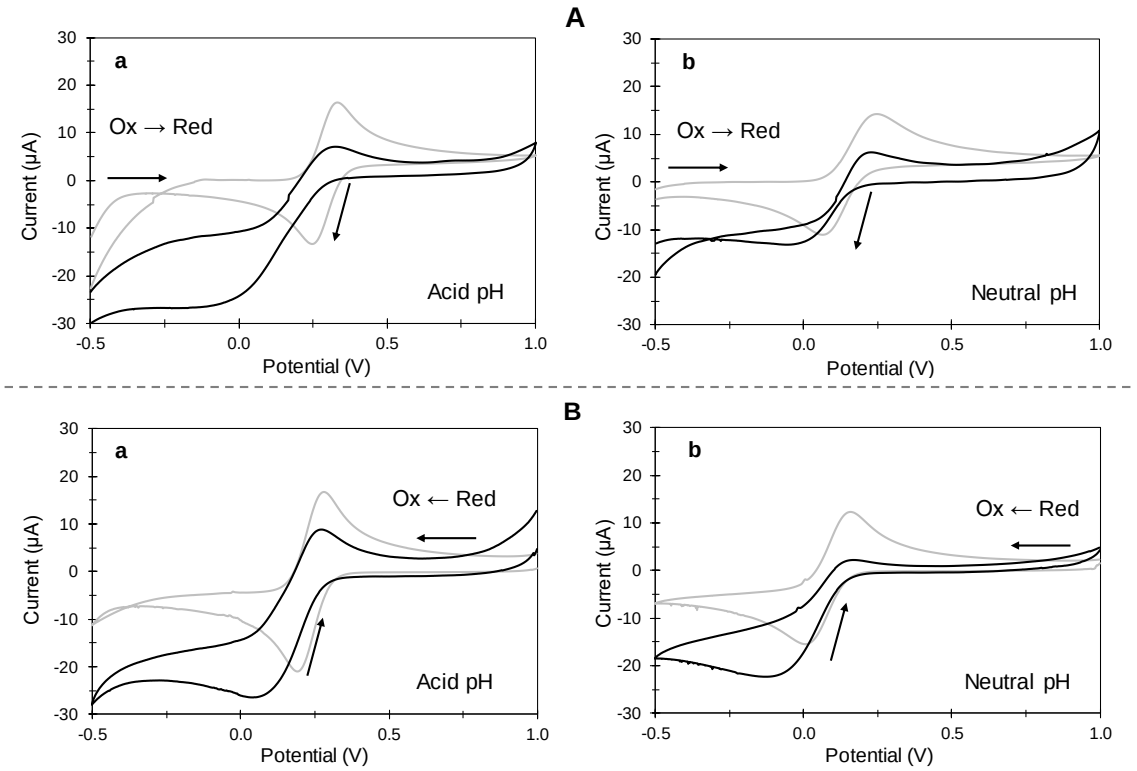

Fig. 2. CVs for bare (grey line) and PAA-CNPs (9.27×10^{16} NPs/mL)-modified (black line) electrodes in 1 mM solutions of (A) $K_4[Fe(CN)_6]$ and (B) $K_3[Fe(CN)_6]$ prepared in 0.1 M HCl (a) and 0.1 M NaCl (b). Scan range: (A) -0.5 V to +1.0 V; (B) +1.0 V to -0.5 V. Scan rate 50 mV/s.

Such behaviour suggests that PAA-CNPs exert an oxidative effect towards the $Fe(CN)_6^{4-}$ oxidation (**Fig. 2A**) in neutral (**Fig. 2A-b**) and mainly strong acidic medium (**Fig. 2A-a**). In basic medium, the red-ox process was not well defined, neither observing any difference in behaviour in presence of PAA-CNPs (data not shown). The explanation to such behaviour probably relies on the presence of Ce (IV) on the PAA-CNPs modified electrode. Under such conditions $Fe(CN)_6^{4-}$ is quickly chemically oxidized by the strong oxidative Ce (IV) just before starting the electrochemical measurement. This effect is more relevant in acidic medium, which is in line with that found in previous studies about the oxidative ability of CNPs towards other reactions like oxidase-related ones **[29,31]**. After that, the chemically generated $Fe(CN)_6^{3-}$ is electrochemically reduced at the initial potential of - 0.5 V, which is in agreement with the high negative current recorded at such potential. The lower oxidation peak current

when scanning from - 0.5 V to + 1.0 V (compared with that of the bare electrode) is also supporting our hypothesis about the so-called CE mechanism (chemical oxidation preceding a charge transfer).

When analysing a solution of the oxidized specie ($Fe(CN)_6^{3-}$) and scanning from positive to negative potentials (from +1.0 V to -0.5 V) (**Fig. 2B**) the reaction mechanism is hypothesized to be ECE type (chemical oxidation between two charge transfer reactions). $Fe(CN)_6^{3-}$ is first electrochemically reduced to $Fe(CN)_6^{4-}$ followed by $Fe(CN)_6^{4-}$ chemical oxidation by the effect of the Ce (IV) present on the electrode, generating more $Fe(CN)_6^{3-}$ which is simultaneously reduced. As in the case of $Fe(CN)_6^{4-}$, no oxidative effect was observed in sodium hydroxide medium (data not shown), while this effect is evident in neutral (**Fig. 2B-b**) and mostly acid (**Fig. 2B-a**) conditions.

3.3. Electrochemical quantification of PAA-CNPs

$K_4[Fe(CN)_6]$ oxidation/reduction process in neutral pH was selected for the quantification studies, avoiding the use of acidic media that would represent an additional step/reagent in further applications in bioanalysis. The effect of the PAA-CNPs concentration on the voltammetric behaviour discussed at **Section 3.2** was first studied, finding that the initial value of the measured negative current increased with the NP concentration (**Fig. 3A**). The results obtained show that, if an adequate potential is fixed (0 V found as optimum; optimization not shown), the intensity of the current recorded in chronoamperometric mode (selected for the quantification studies because of its greater sensitivity, simplicity and speed) during the stage of the chemically generated $Fe(CN)_6^{3-}$ electroreduction (**Fig. 3B**) can be related to the absence (curve a) or presence (curves b-i) of PAA-CNPs on the electrode surface. A proportional increase of oxidative current was observed with corresponding increases in the concentration of PAA-CNPs (from 3.71×10^{13} to 1.85×10^{15} NPs/mL).

It is worthy to note that the higher sensitivity of the chronoamperometry allows the quantification of low PAA-CNPs concentrations that were not detected by cyclic voltammetry. The absolute value of the current generated at 10 s was chosen as the analytical signal and used for quantification of the PAA-CNPs.

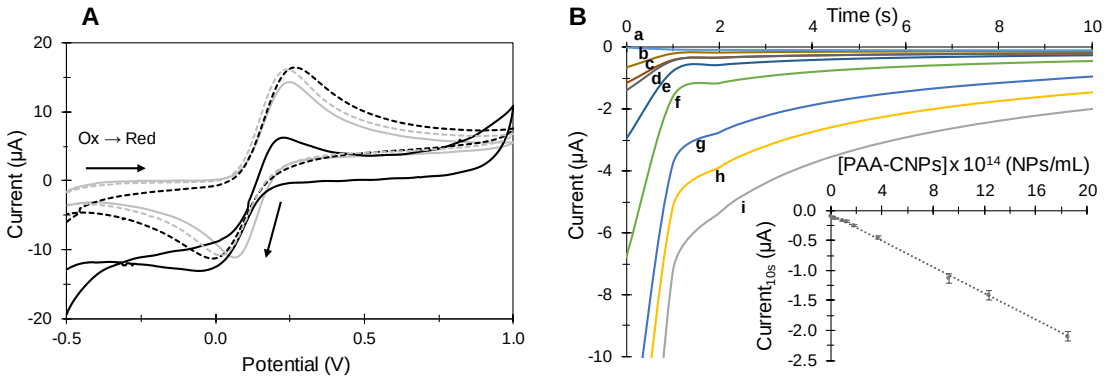

Fig. 3. A) CVs for bare (grey solid line) and PAA-CNPs (9.27×10^{14} NPs/mL grey dotted line, 1.85×10^{15} NPs/mL black dotted line, 9.27×10^{16} NPs/mL black solid line)-modified electrode in 1 mM $K_4[Fe(CN)_6]$ / 0.1 M NaCl. Scan range: -0.5 V to +1.0 V; scan rate 50 mV/s. B) Chronoamperograms recorded at 0 V for increasing PAA-CNPs concentrations: 0 (a), 3.71×10^{13} (b), 9.27×10^{13} (c), 1.24×10^{14} (d), 1.85×10^{14} (e), 3.71×10^{14} (f), 9.27×10^{14} (g), 1.24×10^{15} (h), 1.85×10^{15} NPs/mL (i). Inset: Calibration plot of PAA-CNPs.

A linear relationship between the analytical signal and the PAA-CNPs concentration was found in the range between 3.71×10^{13} and 1.85×10^{15} NPs/mL, with a correlation coefficient of 0.9994 (n = 3), according to the following equation:

$$\text{Current}_{10s}\ (\mu A) = -1.10 \times 10^{-15}\ [\text{PAA-CNPs}]\ (\text{NPs/mL}) - 0.08$$

A limit of detection (LOD, calculated as three times the standard deviation of the intercept divided by the slope and expressed in absolute value) was found to be 3.15×10^{13} NPs/mL. The method shows a reproducibility (RSD) of 4% (n = 3) for a PAA-CNPs concentration of 1.85×10^{15} NPs/mL.

4. Conclusions

Stable suspensions of 3 nm-sized poly (acrylic acid)-coated nanoceria (PAA-CNPs) have been successfully synthesized and characterized by DLS, HR-TEM and ICP-MS analysis. Cyclic voltammetry measurements showed that the PAA-CNPs exert an oxidative effect towards $Fe(CN)_6^{4-}$ oxidation in both acid and neutral pH. Such effect is approached for NPs quantification in chronoamperometric mode, achieving a detection limit of 3.15×10^{13} NPs/mL. Under such conditions, PAA-CNPs can be quantified over two orders of magnitude (3.71×10^{13} and 1.85×10^{15} NPs/mL) with a good reproducibility (RSD: 4%). To the best of our knowledge, this is the first time that such property of PAA-CNPs is studied and applied for quantification purposes. The proposed detection method does not require the chemical agents used in most existing assays for the detection of NP tags. We envisage that this methodology could open the way to further use of PAA-CNPs tags in biosensing as advantageous alternative to enzymes, in terms of stability and cost of the assay **[32–34]**.

Acknowledgements

This work was supported by the FC-GRUPIN-IDI/2018/000166 project from the Asturias Regional Government and the CTQ2017-86994-R and CTQ2014-58826-R projects from the Spanish Ministry of Economy and Competitiveness (MINECO). A. Iglesias-Mayor thanks the Spanish Ministry of Education, Culture and Sports (MECD) for the award of a FPU Grant (FPU2014/04686). A. de la Escosura-Muñiz acknowledges the Spanish Ministry of Science, Innovation and Universities (MICINN) for the "Ramón y Cajal" Research Fellow (RyC-2016-20299). Authors thank to Pablo Llano-Suarez for performing the ICP-MS analysis.

References

[1] N.N. Greenwood, A. Earnshaw, Chemistry of the Elements, Second, 1997.

[2] K. Reed, A. Cormack, A. Kulkarni, M. Mayton, D. Sayle, F. Klaessig, B. Stadler, Exploring the properties and applications of nanoceria: is there still plenty of room at the bottom?, Environ. Sci. Nano. 1 (2014) 390–405. doi:10.1039/C4EN00079J.

[3] A. Karakoti, S. Singh, J.M. Dowding, S. Seal, W.T. Self, Redox-active radical scavenging nanomaterials, Chem. Soc. Rev. 39 (2010) 4422–4432. doi:10.1039/b919677n.

[4] T. Pirmohamed, J.M. Dowding, S. Singh, B. Wasserman, E. Heckert, A.S. Karakoti, J.E.S. King, S. Seal, W.T. Self, Nanoceria exhibit redox state-dependent catalase mimetic activity, Chem. Commun. 46 (2010) 2736–2738. doi:10.1039/b922024k.

[5] C. Xu, X. Qu, Cerium oxide nanoparticle: a remarkably versatile rare earth nanomaterial for biological applications, NPG Asia Mater. 6 (2014) 1–16. doi:10.1038/am.2013.88.

[6] H. Gu, M.D. Soucek, Preparation and characterization of monodisperse cerium oxide nanoparticles in hydrocarbon solvents, Chem. Mater. 19 (2007) 1103–1110. doi:10.1021/cm061332r.

[7] H. Lin, C. Wu, R. Chiang, Facile synthesis of CeO2 nanoplates and nanorods by [100] oriented growth, J. Colloid Interface Sci. 341 (2010) 12–17. doi:10.1016/j.jcis.2009.04.047.

[8] T.S. Sreeremya, K.M. Thulasi, A. Krishnan, S. Ghosh, A novel aqueous route to

fabricate ultrasmall monodisperse lipophilic cerium oxide nanoparticles, Ind. Eng. Chem. Res. 51 (2012) 318–326. doi:10.1021/ie2019646.

[9] S. Sathyamurthy, K.J. Leonard, R.T. Dabestani, M.P. Paranthaman, Reverse micellar synthesis of cerium oxide nanoparticles, Nanotechnology. 16 (2005) 1960–1964. doi:10.1088/0957-4484/16/9/089.

[10] S.M. Hirst, A.S. Karakoti, R.D. Tyler, N. Sriranganathan, S. Seal, C.M. Reilly, Anti-inflammatory properties of cerium oxide nanoparticles, Small. 5 (2009) 2848–2856. doi:10.1002/smll.200901048.

[11] A.S. Karakoti, S. Singh, A. Kumar, M. Malinska, S.V.N.T. Kuchibhatla, K. Wozniak, W.T. Self, S. Seal, PEGylated nanoceria as radical scavenger with tunable redox chemistry, J. Am. Chem. Soc. 131 (2009) 14144–14145. doi:10.1021/ja9051087.

[12] J.M. Perez, A. Asati, S. Nath, C. Kaittanis, Synthesis of biocompatible dextran-coated nanoceria with pH-dependent antioxidant properties, Small. 4 (2008) 552–556. doi:10.1002/smll.200700824.

[13] X. Li, L. Sun, A. Ge, Y. Guo, Enhanced chemiluminescence detection of thrombin based on cerium oxide nanoparticles., Chem. Commun. 47 (2011) 947–949. doi:10.1039/c0cc03750h.

[14] J.T. Dahle, Y. Arai, Environmental geochemistry of cerium: applications and toxicology of cerium oxide nanoparticles, Int. J. Environ. Res. Public Health. 12 (2015) 1253–1278. doi:10.3390/ijerph120201253.

[15] C.T. Campbell, C.H.F. Peden, Oxygen vacancies and catalysis on ceria surfaces, Science (80-.). 309 (2005) 713–714. doi:10.1126/science.1113955.

[16] D. Andreescu, G. Bulbul, R.E. Özel, A. Hayat, N. Sardesai, S. Andreescu, Applications and implications of nanoceria reactivity: measurement tools and environmental impact, Environ. Sci. Nano. 1 (2014) 445–458. doi:10.1039/C4EN00075G.

[17] L.F. Arenas, C. Ponce De León, F.C. Walsh, Electrochemical redox processes involving soluble cerium species, Electrochim. Acta. 205 (2016) 226–247. doi:10.1016/j.electacta.2016.04.062.

[18] C. Korsvik, S. Patil, S. Seal, W.T. Self, Superoxide dismutase mimetic properties exhibited by vacancy engineered ceria nanoparticles, Chem. Commun. 0 (2007) 1056–1058. doi:10.1039/b615134e.

[19] E.G. Heckert, A.S. Karakoti, S. Seal, W.T. Self, The role of cerium redox state in the SOD mimetic activity of nanoceria, Biomaterials. 29 (2008) 2705–2709. doi:10.1016/j.biomaterials.2008.03.014.

[20] X. Jiao, H. Song, H. Zhao, W. Bai, L. Zhang, Y. Lv, Well-redispersed ceria nanoparticles: promising peroxidase mimetics for H2O2 and glucose detection, Anal. Methods. 4 (2012) 3261–3267. doi:10.1039/c2ay25511a.

[21] Z. Li, X. Yang, Y. Yang, Y. Tan, Y. He, M. Liu, X. Liu, Q. Yuan, Peroxidase-mimicking nanozyme with enhanced activity and high stability based on metal-support interaction, Chem. - A Eur. J. 24 (2018) 409–415. doi:10.1002/chem.201703833.

[22] M.H. Kuchma, C.B. Komanski, J. Colon, A. Teblum, A.E. Masunov, B. Alvarado, S. Babu, S. Seal, J. Summy, C.H. Baker, Phosphate ester hydrolysis of biologically relevant molecules by cerium oxide nanoparticles, Nanomedicine Nanotechnology, Biol. Med. 6 (2010) 738–744. doi:10.1016/j.nano.2010.05.004.

[23] I. Celardo, J.Z. Pedersen, E. Traversa, L. Ghibelli, Pharmacological potential of cerium oxide nanoparticles, Nanoscale. 3 (2011) 1411–1420. doi:10.1039/C0NR00875C.

[24] M. Ornatska, E. Sharpe, D. Andreescu, S. Andreescu, Paper bioassay based on ceria nanoparticles as colorimetric probes, Anal. Chem. 83 (2011) 4273–4280. doi:10.1021/ac200697y.

[25] A.S. Karakoti, O. Tsigkou, S. Yue, P.D. Lee, M.M. Stevens, J.R. Jones, S. Seal, Rare earth oxides as nanoadditives in 3-D nanocomposite scaffolds for bone regeneration, J. Mater. Chem. 20 (2010) 8912–8919. doi:10.1039/c0jm01072c.

[26] C. Mandoli, F. Pagliari, S. Pagliari, G. Forte, P. Di Nardo, S. Licoccia, E. Traversa, Stem cell aligned growth induced by CeO2 nanoparticles in PLGA scaffolds with improved bioactivity for regenerative medicine, Adv. Funct. Mater. 20 (2010) 1617–1624. doi:10.1002/adfm.200902363.

[27] C. Xu, Y. Lin, J. Wang, L. Wu, W. Wei, J. Ren, X. Qu, Nanoceria-triggered synergetic drug release based on CeO2-capped mesoporous silica host-guest interactions and switchable enzymatic activity and cellular effects of CeO2, Adv. Healthc. Mater. 2 (2013) 1591–1599. doi:10.1002/adhm.201200464.

[28] M. Li, P. Shi, C. Xu, J. Ren, X. Qu, Cerium oxide caged metal chelator: anti-aggregation and anti-oxidation integrated H2O2-responsive controlled drug release for potential Alzheimer's disease treatment, Chem. Sci. 4 (2013) 2536–2542. doi:10.1039/C3SC50697E.

[29] A. Asati, C. Kaittanis, S. Santra, J.M. Perez, pH-tunable oxidase-like activity of cerium oxide nanoparticles achieving sensitive fluorigenic detection of cancer biomarkers at neutral pH, Anal. Chem. 83 (2011) 2547–2553.

doi:10.1021/ac102826k.

[30] A. Asati, S. Santra, C. Kaittanis, S. Nath, J.M. Perez, Oxidase-like activity of polymer-coated cerium oxide nanoparticles, Angew. Chemie Int. Ed. 48 (2009) 2308–2312. doi:10.1002/anie.200805279.

[31] H. Cheng, S. Lin, F. Muhammad, Y.W. Lin, H. Wei, Rationally modulate the oxidase-like activity of nanoceria for self-regulated bioassays, ACS Sensors. 1 (2016) 1336–1343. doi:10.1021/acssensors.6b00500.

[32] S. Singh, Cerium oxide based nanozymes: redox phenomenon at biointerfaces, Biointerphases. 11 (2016) 04B202. doi:10.1116/1.4966535.

[33] G. Wang, J. Zhang, X. He, Z. Zhang, Y. Zhao, Ceria nanoparticles as enzyme mimetics, Chinese J. Chem. 35 (2017) 791–800. doi:10.1002/cjoc.201600845.

[34] Y. Zhou, B. Liu, R. Yang, J. Liu, Filling in the gaps between nanozymes and enzymes: challenges and opportunities, Bioconjug. Chem. 28 (2017) 2903–2909. doi:10.1021/acs.bioconjchem.7b00673.